Satellite Clock and Ephemeris Error Bounding Characterization for Galileo and Estimated CNAV

Xinwei Liu, Rebecca Wang, Juan Blanch, Todd Walter,

Stanford University

BIOGRAPHY

Xinwei Liu is an Engineer's Degree candidate at the GPS laboratory at Stanford University.

Rebecca Wang is a Ph.D. candidate at the GPS laboratory at Stanford University.

Juan Blanch is a senior research engineer at the GPS laboratory at Stanford University.

Todd Walter is a Professor of Research and director of the GPS laboratory at Stanford University.

ABSTRACT

The Advanced Receiver Autonomous Integrity Monitoring (ARAIM) concept relies on characterizing the satellite clock and ephemeris bounding parameters. In this paper, we expand on the previous study on the GPS error bounding parameters to include Galileo and the approximation of the bounding parameters of the Civil Navigation (CNAV) Message type. In particular, we compute the bounding parameters that capture their inherent variability. We then partition the error by their observable conditions to determine whether the currently collected data is representative of future error behavior. Furthermore, for Galileo, we change the nominal error definition to investigate how it would affect the bounding parameter distribution. We find that the Galileo normalized error data are bounded with Gaussian with mean of 0.04 and standard deviation of 0.04 for different partitions with newer satellites having more stable and lower bounding parameters. Lowering the nominal error definition threshold stabilizes the bounding parameters. We estimate the CNAV bounding parameter by lowering the σURA values. We find the normalized errors are bounded with Gaussian with mean of 0.41 and standard deviation of 1.15 even after lowering the σ_{URA} values. In addition, lowering the σ_{URA} values stabilizes the bounding parameters.

I. INTRODUCTION

The characterization of the GPS satellite clock and ephemeris nominal error bounding parameters is crucial for the concept of Advanced Receiver Autonomous Integrity Monitoring(ARAIM). In a previous study, we investigated such parameter behavior for the Legacy Navigation (LNAV) message type. We applied three bounding methods to the GPS satellite clock and ephemeris nominal error utilizing a Gaussian bounding algorithm(1). The bounding algorithm outputs two parameters, the Gaussian mean, $bias$, and the Gaussian standard deviation, σ. We used 200 user projected errors (UPE), and the algorithm computed $bias$ by finding the smallest $bias$ that works for all the users and then computes the largest σ for all the users corresponding to this $bias$.The first bounding method directly applied the Gaussian bounding algorithm to the UPE. We referred to it as the two-step bounding algorithm. The second algorithm simplified the first algorithm to reduce the computational cost. We referred to it as the direct bounding algorithm. The third algorithm output a single set of bounding parameters that captures the inherent variability in the bounding parameters computed using the bootstrap method (2). We referred to it as the bootstrap bounding algorithm. In the previous study, using the data from 2008 to 2022, we found that the bounding parameters provided by the three bounding algorithms are close to each other. We concluded that it might be possible to use the two-step bounding algorithm, which is computationally cheap, to replace the bootstrap bounding algorithm, which captures the inherent variability in the bounding parameters at a higher computation cost. In addition, we partitioned the data using different observable conditions to explore how representative the collected data are for future error data yet to be collected. Finally, we examine how including the near-fault data points as faulted affects the bounding parameters.

In this study, we expand the constellation to Galileo and apply the same analysis to Galileo data from 2018 to 2022. We examine how fault definition affects the observed fault probability and the bounding parameters, which was briefly discussed in the previous study(2). In addition, as Civil Navigation (CNAV) message will be used for ARAIM, we apply an approximation to the CNAV message type and characterize its error bounding parameter behavior as we did for the LNAV message.

We first review the mathematics for the bounding parameter formulation in section II. Then we present the bounding parameter

behavior results for Galileo and the approximation of CNAV, respectively, in section III. For each data set, we also evaluate how different fault definitions affect the fault rate and the bounding parameters. The experimental results are provided in section IV.

II. BOOTSTRAP SINGLE GAUSSIAN BOUNDING PARAMETER

In the previous study, we introduced a way to calculate a single set of bounding parameters that captures the inherent variability of the satellite clock and ephemeris error bounding parameters. In our problem, we apply a Gaussian bounding algorithm to compute the statistics of the Gaussian distribution, whose tail bounds over the probability of the absolute error value larger than some value L. The formulation is shown in Equation 1

$$P(|\varepsilon| > L) \leq 2 \times (1 - Q(\frac{L - bias}{\sigma})) \tag{1}$$

Here, P is the probability, ε is the error, Q is the Gaussian CDF, $bias$ is the Gaussian mean, and σ is the Gaussian standard deviation. Utilizing the bootstrap method, we obtain the empirical probability distribution of the error bounding parameters. We then incorporate the probability distribution into a single set of bounding parameters, as shown in Equation 2

$$\frac{L - Bias}{\Sigma} = Q^{-1}\left(\frac{1}{N}\sum_{i=1}^{N} Q\left(\frac{L - bias(i)}{\sigma(i)}\right)\right) \tag{2}$$

Here, $Bias$ and Σ are the bounding parameters that capture the inherent variability. N is the number of bootstrap samples. $bias(i)$ and $\sigma(i)$ correspond to each bootstrap sample's bounding parameters. As a result, the bounding parameters $Bias$ and Σ capture the variability calculated in the bootstrap process. We then find the set of $(Bias, \Sigma)$ that would work for all the possible L values. Picking the $Bias$ to be the bounding parameter calculated by directly applying the bounding parameter to the original error data, we obtain Σ as we did in (2).

III. GALILEO AND ESTIMATED CIVIL NAVIGATION (CNAV) MESSAGE

In the previous study, we bounded the UPE values for GPS from 2008 to 2022. We explored the variability of the bounding parameter computed in equation 2 for different observable conditions for LNAV message type(2). This approach allows us to examine the stability of the bounding parameters for different observable conditions and how representative the current bounding parameters are for the error data yet to be collected. Suppose the bounding parameter values are close for different observable condition values. In that case, we can speculate that the parameters are stable for the given data and likely to be representative of error data corresponding to observable condition values yet to be collected. For example, taking the observable condition to be time, we compute the bounding parameters for different time periods and compare their values. This comparison allows us to analyze how the bounding parameters vary with time and to speculate how the bounding parameters might behave in the future. In addition, we compared the bounding parameter values obtained using the bounding algorithm directly against the bootstrap bounding parameters. The result shows that the two bounding methods provide similar bounding parameter values, which implies that for this particular set of data, it might be possible to replace the bootstrap bounding parameters, which capture the inherent variability with the two-step bounding parameters, which are computationally cheap (2). In this study, we expand our error data set to Galileo and message types to explore how changing the definition of the nominal error would affect the bounding parameter behavior.

1. Constellation Expansion

In this study, we seek to expand this method to other GNSS constellations, particularly Galileo, which will be included as a part of the ARAIM. We take the available Galileo data and partition the data by time window and satellite vehicle number to examine how the bounding parameters vary with different observable condition values to conclude the bounding parameter stability. In doing so, we determine whether the parameters for the collected errors are representative of the bounding parameters of the error data yet to be collected. We also examine how close the outputs of the three bounding methods are, as we did for GPS.

2. Navigation Message Expansion

We also want to explore the bounding parameter behavior from the Civil Navigation Message(CNAV), which will be used in ARAIM, through the L5 signals. We use the LNAV message to approximate the L5 signal in our study. We know the CNAV message type has a lower σ_{URA} than LNAV(3)(4). To approximate the CNAV bounding parameters, we take the LNAV clock and ephemeris data points corresponding to $\sigma_{URA} = 2.40meters$, normalize them with lower σ_{URA} values and find the nominal error with a threshold of 4.42. In this sense, we have "inflated" the normalized error data values. We see tighter error

bounds with the different σ_{URA} values. The results are shown in the next section.

3. Nominal Error Definition Modification

Lowering the σ_{URA} would change the definition of the nominal errors. The nominal clock and ephemeris errors are defined as the error with a value below $4.42 \times \sigma_{URA}$, where σ_{URA} is the User Range Accuracy. The P_{sat} value for GPS is 10^{-5} (5), which establishes the maximum percentage of data that can be considered faulty. In the previous study, we observed that by lowering this threshold from 4.42 to 3, we obtained more stable behavior for the bounding parameters for different observable condition values. In this sense, lowering the threshold "stabilizes" the bounding parameters. For Galileo, the nominal error is defined with a threshold of $4.17 \times \sigma_{URA}$. The P_{sat} is 3×10^{-5} . In this study, we seek to set the threshold to a lower value for Galileo such that the fraction of data eliminated is less than P_{sat}. For Galileo, we set the threshold to be $2 \times \sigma_{ura}$ such that the data eliminated is slightly smaller than 10^{-5} for the new definition of faulty data points.

In the following section, we present Galileo analysis and CNAV approximation results, respectively.

IV. EXPERIMENT

This section presents the experimental result for the above three analyses. We present the result for Galileo and its nominal error bounding definition analysis. In particular, we plot the two-step, direct, and bootstrap bounding parameters with different observable condition values. We then apply the same analysis to approximated CNAV using a σ_{URA}approximation.

1. Galileo

In the Galileo plot analysis, we aim to do the following. First, justify the bootstrap simplification. Second, justify the two-step bounding parameter substitution. Third, explore the bounding parameter variability with different observable condition values. Fourth, explore the effect of fault definition change. Fifth, examine whether the parameters are below the normalization. Sixth, examine whether the $bias$ values are small. We elaborate on the motivation for the first four objectives. For the first objective, in (2), to reduce the computational cost of the bootstrap method used to compute the bootstrap bounding σ, we replaced the two-step bounding parameters with the direct bounding parameters. If we observe that the two-step and the direct bounding parameters are close, we are motivated to apply this simplification to the bootstrap bounding parameters. For our plot, this result corresponds to the blue and red dots being close to each other. For the second objective, suppose the two-step and the direct bounding parameters are close to the bootstrap bounding parameters. We can use the two-step bounding parameter to capture the inherent variation of the bounding parameters explored using the bootstrap bounding parameters for the data set. We are motivated to apply this substitution due to the high computation cost of the bootstrap bounding method. If such a substitution is justified, we can capture the bounding parameter's inherent variability without wasting additional computational power for the given data. For the third objective, we observe how the bounding parameters vary with different observable condition values, as described in section III. Suppose the bounding parameter values are close to each other for different observable condition values. In that case, we can conclude that the parameters are "stable" for the given data and can use the computed values to infer the bounding parameter for data yet to be collected. Finally, we can explore how lowering the fault definition threshold changes the bounding behavior. In (2), we saw that the bounding parameters became more stable after lowering the threshold.

We take the Galileo user projected error from 2018 to 2022. The data is taken every 5 minutes. We define the faulted data as values larger than $\sigma_{URA} \times 4.17$ and $\sigma_{URA} \times 2$ to explore the effect of fault definition. In this case, as applied in (2), we plot the bounding parameters against different observable condition values.

We first compute the bounding parameters against different time periods. The time period window is taken to be 1 year, and we slide this window by every 6 months. The result is shown in Figure 1

Here, we plot the three sets of bounding parameters as introduced in (2) and the introduction section. The blue dots are the direct bounding σs computed using the designated 1 year of data. The red dots are the two-step bounding σs computed using the designated 1 year of data. The green dots are the bootstrap bounding σs computed using the statistics formulated in section II.

For this study, we set the $bias$ values to be the same for better σ comparisons. We observe that all three bounding methods produce similar σ values. This result justifies the bootstrap simplification for the given data set. It implies that it might be possible to use the two-step bounding method to capture the inherent variability in the bounding parameters. Furthermore, we observe that σ values decrease with time, except for 2019. The bounding parameter variation with different observable condition values becomes less obvious after lowering the threshold. In addition, all the bounding parameters are below the normalization with small $bias$ values.

We then explore the variation with different satellite vehicle numbers (SVN). The results are plotted in figure 2

As we can observe from the plot, the bounding parameters are close. All the parameters are below the normalization. The newer

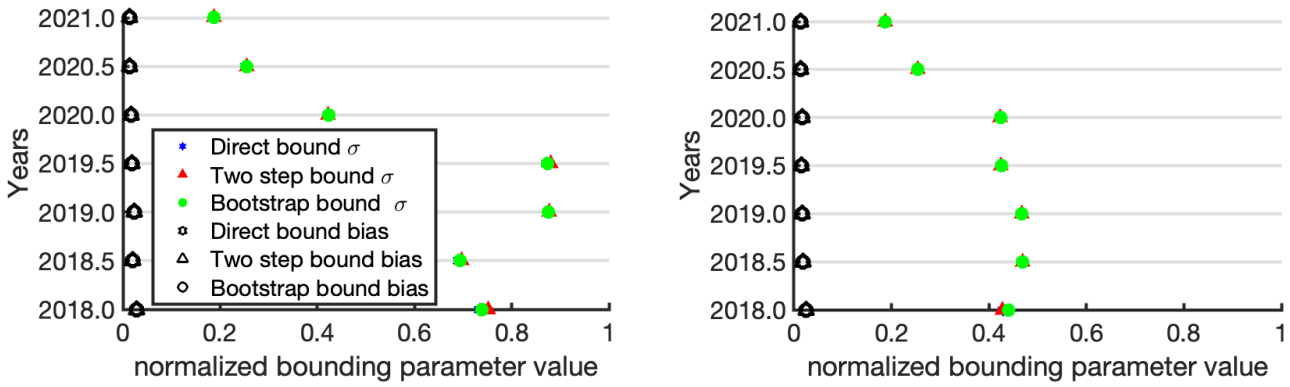

(a) nominal error bounding parameters $\sigma_{URA} \times 4.17$

(b) nominal error bounding parameters $\sigma_{URA} \times 2$

Figure 1: Bounding parameter results for direct, two-step, and bootstrap bounding processes varying in time. The blue dots are the direct bounding σs computed using the designated 1 year of data. The red dots are the two-step bounding σs computed using the designated 1 year of data, and the green dots are the bootstrap bounding σs computed using the abovementioned method. The black circles are the biases. Since we set them to be the same for the three bounding methods, they overlap.

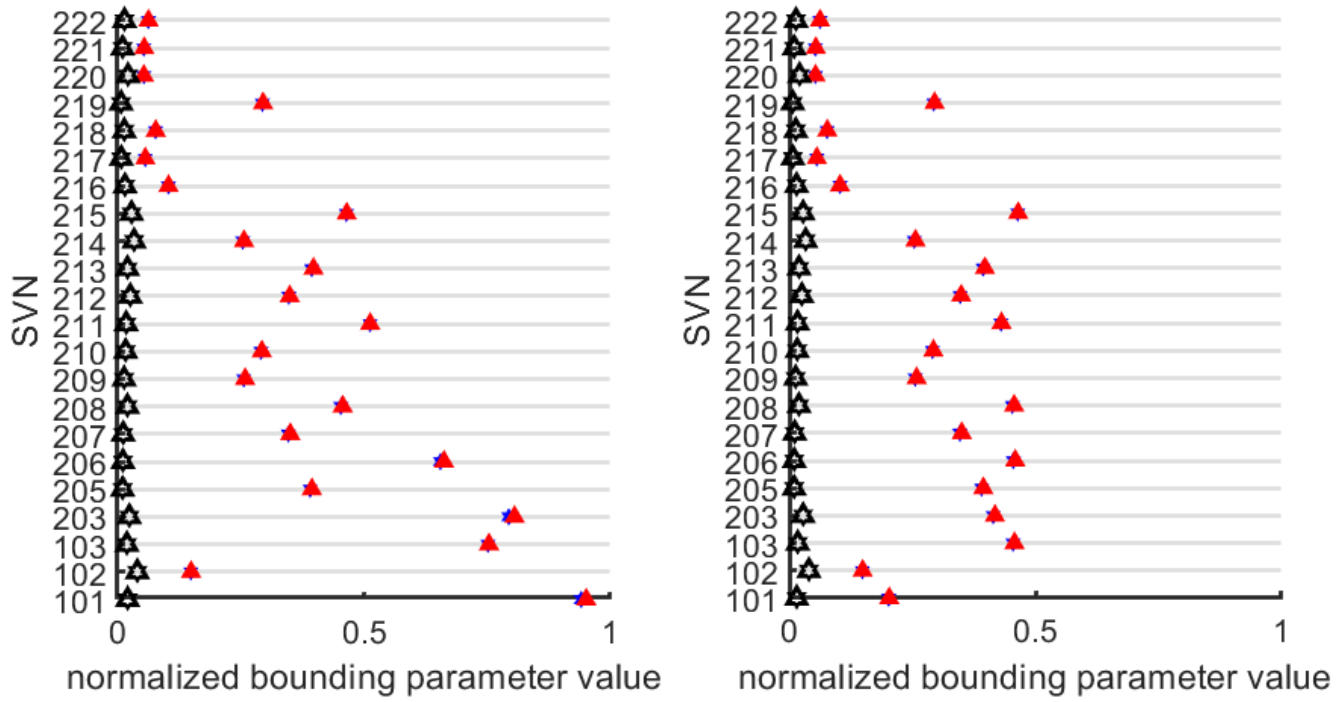

(a) nominal error bounding parameters $\sigma_{URA} \times 4.17$

(b) nominal error bounding parameters $\sigma_{URA} \times 2$

Figure 2: Bounding parameter results for direct and two-step bonding processes varying in SVN. The blue dots are the direct bounding σs computed using the designated 1 year of data. The red dots are the two-step bounding σs computed using the designated 1 year of data. The black circles are the biases. Since we set them to be the same for two bounding methods, they overlap.

satellites have lower σ values compared to older satellites. After lowering the threshold, the σ values become more stable. All the parameters are below normalization, and the bias values are small. We now move on to the analysis for approximated CNAV.

2. Approximated CNAV

To approximate the CNAV bounding parameters, we take the LNAV message data used in (2) for GPS from 2008 to 2022, taken every 15 minutes, and lower the σ_{URA} values. Specifically, we select the LNAV clock and ephemeris errors with $\sigma_{URA} = 2.4 meters$ and normalize them by lower σ_{URA}. We first explore the appropriate σ_{URA} values that are reasonable for our study by computing the bounding parameters for all the given data after changing the σ_{URA}. This analysis uses the nominal error defined as the error value less than $4.42 \times \sigma_{URA}$.In figure 3. we plot the bounding parameter values against different σ_{URA} normalizations. Here we ignored the bootstrap analysis and plotted the direct and the two-step bounding parameters. As we can

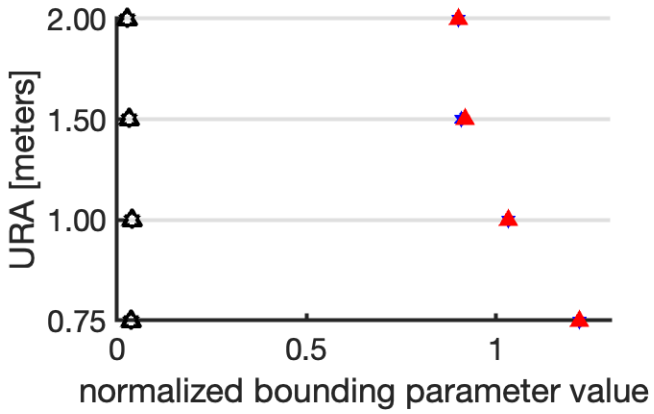

Figure 3: nominal error bounding parameters for different $\sigma_{URA} values$

observe from the plot, the bounding exceeds the normalization for σ_{URA} values lower than 1. We, therefore, pick values to be 2 and 1.5 meters. However, as our result is a conservative approximation of the true CNAV error, this plot does not indicate that for true CNAV error, the σ_{URA} can only go to 1.5 meters. One should refrain from drawing direct conclusions regarding how low the CNAV error's σ_{URA} can go based on this study.

We now compute the bounding parameter values for each observable condition value. Since the computation is carried out by finding the smallest bounding $bias$ that works for all the users and then finding the σ that works for all the users for that $bias$ value, we need to guarantee that each user, for the given observable condition, can provide enough data to generate a statistically significant result. For our case, we discard the UPE value corresponding to a specific user and specific observable condition if the amount of data is less than 10000 data points, which is approximately 3 months' worth of data. For these plots, we focus on four potential findings. First, we explore the differences between bounding parameters generated from different bounding algorithms, namely the two-step and the direct bounding algorithms. Second, we explore how bounding parameters vary with different observable condition values. Third, we examine how lowering the σ_{URA} impacts the bounding parameters. Fourth, we examine if the $bias$ values are small. Finally, we determine whether any of the bounding parameters exceed the normalization.

We first plot results varying time period for σ_{URA} of 2 and 1.5 meters in figure 4. The time window is three years and is slid every 1 year.

Here we can see that the two-step and the direct bounding σs have negligible differences for a given time window. The σ values have a decreasing trend and were only larger from 2019 to 2022. In addition, we observe that lowering the σ_{URA} values, although "inflates" the data, also stabilizes the data as we observe less variation in the σ values among the different time windows. After inflating the data, applying the same threshold allows the algorithm to filter out more data, thus, stabilizing the bounding parameters. One can also examine this effect by looking at the threshold value. We can consider the error values prior to normalization. We have $threshold = 4.42 \times \sigma_{URA}$.As we lower the σ_{URA} value, the threshold value is also lowered, causing more data to be eliminated. As a direct result of the data elimination, the bounding parameter values become "uniform" or stable. Another observation we can make is that all the bounding parameters are below the normalization, and the $bias$ values are small.

Moving onto the analysis for different SVNs. We plot the result in figure 5

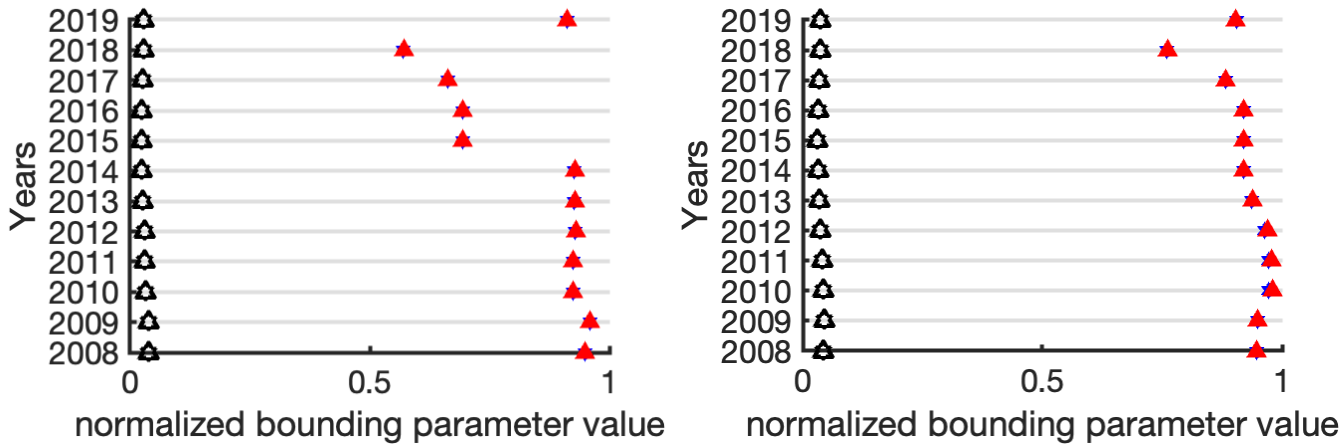

(a) nominal error bounding parameters $\sigma_{URA} = 2meters$

(b) nominal error bounding parameters $\sigma_{URA} = 1.5meters$

Figure 4: Normalized GPS bounding parameters vary by time from 2008 to 2022 with time window of 3 years and slide every 1 year plotted for different σ_{URA} values

Here the two-step and the direct bounding σs difference are small for a given SVN. The σ values do not have a general trend, with several exceeding the normalization. The effect of lowering the σ_{URA} value is not obvious. For $\sigma_{URA} = 2meters$, SVN 26,35,38,39,40,and 73 exceed the normalization. For $\sigma_{URA} = 1.5m$, SVN 24,26,27,30,35,36,38,39,40,52, and 61 exceed the normalization. In addition, the $bias$ values are relatively large for SVN 24, 25, 27, 35, 47, 57, 52, and 61. SVN 24, 25, 27,52, and 61 have biased UPE data. Their mean is larger than the others. SVN 35, 47, and 57 have asymmetric distributions, which cause the bounding $bias$s to be larger. In addition, some of the SVNs with smaller numbers suffer from the lack of data due to retirement. Moving onto the satellite block variation. In figure 6, we plot the bounding parameter values against different satellite blocks.

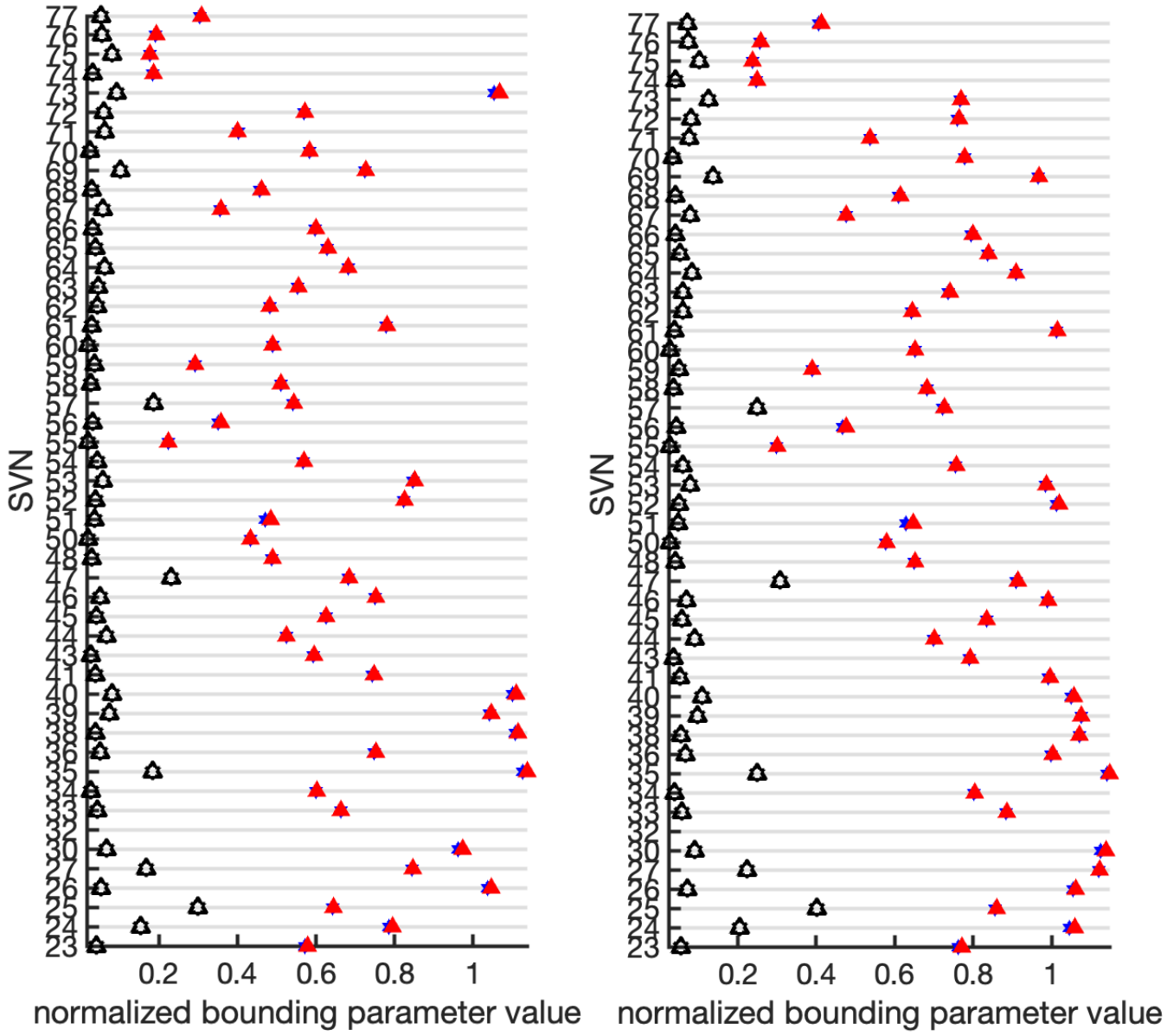

(a) nominal error bounding parameters $\sigma_{URA} = 2meters$

(b) nominal error bounding parameters $\sigma_{URA} = 1.5meters$

Figure 5: Normalized Approximated CNAV bounding parameters vary by SVN from 2008 to 2022 plotted for different σ_{URA} values

Here the two-step and the direct bounding σs difference are small for a given block. The σ values tend to decrease for newer satellite blocks. The bounding parameters are more stable for $\sigma_{URA} = 1.5m$. No block exceeds the normalization for $\sigma_{URA} = 2m$. For $\sigma_{URA} = 1.5m$, block IIA barely exceeds the normalization. In addition, the $bias$ values are small for all blocks.

We also compute the bounding parameter values against different ages of data or times since the last upload (TSLU) for 2013 to 2022. The results are plotted in Figure 7 The two-step and the direct bounding σs difference are small for a given age of

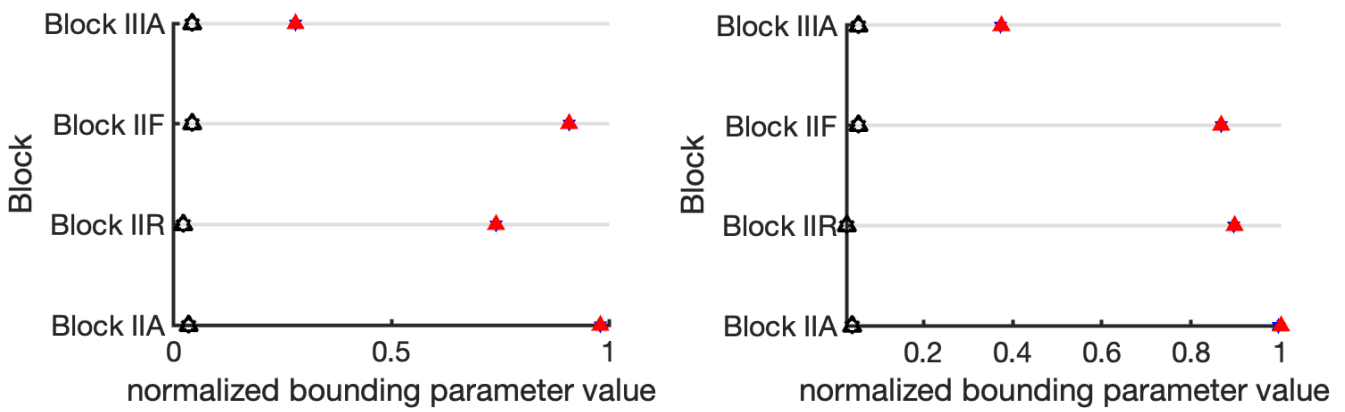

(a) nominal error bounding parameters $\sigma_{URA} = 2meters$

(b) nominal error bounding parameters $\sigma_{URA} = 1.5meters$

Figure 6: Normalized Approximated CNAV bounding parameters vary by satellite blocks from 2008 to 2022 plotted for different σ_{URA} values

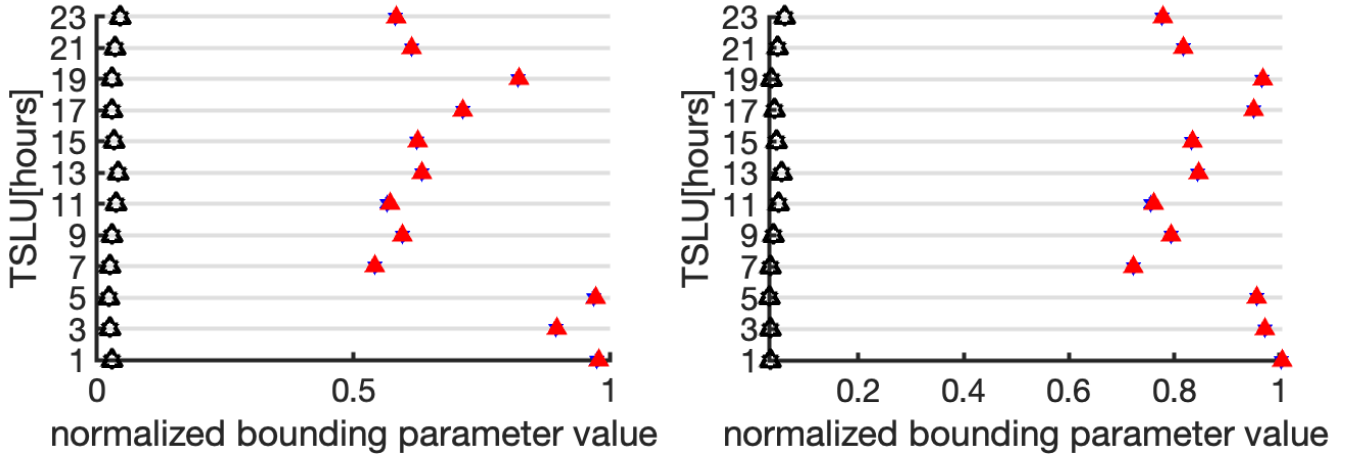

(a) nominal error bounding parameters $\sigma_{URA} = 2meters$

(b) nominal error bounding parameters $\sigma_{URA} = 1.5meters$

Figure 7: Normalized Approximated CNAV bounding parameters vary by TSLU from 2013 to 2022 plotted for different σ_{URA} values

data. There is no apparent trend for how the bounding parameters vary with the age of the data. Lowering the σ_{URA} stabilizes the parameters. No block exceeds the normalization for $\sigma_{URA} = 2m$. For $\sigma_{URA} = 1.5m$, block IIA barely exceeds the normalization. In addition, the $bias$ values are small for all ages of data. Our plot shows safe support even after lowering the σ_{URA} values.

V. CONCLUSION

In this study, we evaluate Galileo's satellite clock and ephemeris error bounding parameter behavior and approximate CNAV error data by lowering the σ_{URA} values. We examine how the bounding parameters change with different observable condition values. For Galileo, we find that the normalized nominal errors are bounded by Gaussian distribution with mean below 1 and standard deviation of 0.04. We showed that different bounding algorithms produce similar bounding parameter values for given observable condition values. This result implies we can use the two-step bounding algorithm, which is computationally cheap to capture the inherent variability of the bounding parameters. We also find that newer satellites tend to generate smaller bounding σ, and the bounding parameters become more stable after eliminating the near-fault data points. Finally, all the bounding

parameters are below the normalization with small $bias$ values. For our CNAV approximation, we find that the normalized nominal errors are bounded by Gaussian distribution with mean below 1 and standard deviation of 0.04. After lowering the σ_{URA} values to 2 and 1.5 meters for LNAV error data, we see that lowering the σ_{URA} stabilizes the bounding parameters. Most of the $bias$ values are small with a few SVN exceptions, and most of the bounding parameters are below the normalization. These results provide valuable insights for the satellite error integrity analysis for ARAIM applications.

ACKNOWLEDGEMENTS

We gratefully acknowledge the support of the FAA for funding this work.

REFERENCES

[1] Blanch, J., Walter, T., amp; Enge, P. (2019). Gaussian bounds of sample distributions for integrity analysis. IEEE Transactions on Aerospace and Electronic Systems, 55(4), 1806–1815. https://doi.org/10.1109/taes.2018.2876583

[2] Liu, X., Wang, R., Blanch, J., amp; Walter, T. (2022). Evaluation of satellite clock and ephemeris error bounding predictability for integrity applications. ION GNSS+, The International Technical Meeting of the Satellite Division of The Institute of Navigation. https://doi.org/10.33012/2022.18306

[3] PNT Technical Director, MilComm PNT Directorate, Space Systems Command(SSC)(2022). IS-GPS 200.https://www.gps.gov/technical/icwg/

[4] PNT Technical Director, MilComm PNT Directorate, Space Systems Command(SSC)(2022). IS-GPS 800.https://www.gps.gov/technical/icwg/

[5] Pullen, S., Lo, S., Katz, A., Blanch, J., Walter, T., Katronick, A., Crews, M., amp; Jackson, R. (2021). Ground monitoring to support araim for military users: Alternatives for rapid and rare update rates. Proceedings of the 34th International Technical Meeting of the Satellite Division of The Institute of Navigation (ION GNSS+ 2021). https://doi.org/10.33012/2021.18159

[6] Liu, X., Blanch, J., amp; Walter, T. (2022). Investigation into satellite clock and ephemeris errors bounding uncertainty and predictability. The International Technical Meeting of the The Institute of Navigation. https://doi.org/10.33012/2022.18206